2016

Role of Securin, Separase and Cohesins in female meiosis and polar body formation in Drosophila

Zhihao Guo
University of Windsor

Osamah Batiha

Mohammed Bourouh
University of Windsor

Eric Fifield
University of Windsor

Andrew Swan
University of Windsor

© 2016. Published by The Company of Biologists Ltd | Journal of Cell Science (2016) 129, 531-542 doi:10.1242/jcs.179358

RESEARCH ARTICLE

Role of Securin, Separase and Cohesins in female meiosis and polar body formation in *Drosophila*

Zhihao Guo, Osamah Batiha*, Mohammed Bourouh, Eric Fifield and Andrew Swan‡

ABSTRACT

Chromosome segregation in meiosis is controlled by a conserved pathway that culminates in Separase-mediated cleavage of the α-kleisin Rec8, leading to dissolution of cohesin rings. *Drosophila* has no gene encoding Rec8, and the absence of a known Separase target raises the question of whether Separase and its regulator Securin (Pim in *Drosophila*) are important in *Drosophila* meiosis. Here, we investigate the role of Securin, Separase and the cohesin complex in female meiosis using fluorescence *in situ* hybridization against centromeric and arm-specific sequences to monitor cohesion. We show that Securin destruction and Separase activity are required for timely release of arm cohesion in anaphase I and centromere-proximal cohesion in anaphase II. They are also required for release of arm cohesion on polar body chromosomes. Cohesion on polar body chromosomes depends on the cohesin components SMC3 and the mitotic α-kleisin Rad21 (also called Vtd in *Drosophila*). We provide cytological evidence that SMC3 is required for arm cohesion in female meiosis, whereas Rad21, in agreement with recent findings, is not. We conclude that in *Drosophila* meiosis, cohesion is regulated by a conserved Securin–Separase pathway that targets a diverged Separase target, possibly within the cohesin complex.

KEY WORDS: *Drosophila*, Meiosis, Sister chromatid cohesion

INTRODUCTION

The proper segregation of chromosomes in mitosis and in meiosis depends on the regulated disassembly of cohesin ring complexes that link sister chromatids. Prior to anaphase, Securin (Pim in *Drosophila*) binds and inhibits the crucial mediator of sister chromatid segregation, Separase (Sse). Securin destruction, mediated by the anaphase-promoting complex/cyclosome (APC/C) ubiquitin ligase, results in the release of active Separase, which then cleaves a crucial component of the cohesin complex, the α-kleisin Rad21 (also called Vtd in *Drosophila*). Cleavage of Rad21 allows sister chromatid separation (reviewed in Nasmyth, 2002). Like the mitotic cyclins, Pim contains D-box and KEN-box motifs that mediate recognition by the APC/C (Leismann et al., 2000; Leismann and Lehner, 2003).

Cohesin complexes can differ in their composition in meiosis compared to mitosis. Most notably, in organisms ranging from yeast to mammals, a meiosis-specific α-kleisin, Rec8, substitutes for Rad21. Like its mitotic counterpart, Rec8 is cleaved by Separase to trigger anaphase (Revenkova and Jessberger, 2005). In meiosis, cohesin release occurs in two steps (reviewed in Revenkova and Jessberger, 2005). First, Rec8 is cleaved on chromosome arms, distal to chiasma. This results in the anaphase I segregation of homologues. Meanwhile, centromere-proximal cohesion is maintained by the activity of Shugoshin (Mei-S332 in *Drosophila*) (Watanabe, 2005). In anaphase II, Rec8 is cleaved on the remaining, centromere-proximal, cohesins. This allows for sister chromatid segregation.

Although broadly conserved in eukaryotes, this pathway appears to differ in *Drosophila*. First, meiotic cohesion in *Drosophila* requires the non-conserved proteins Ord, Sunn and Solo (Bickel et al., 1997, 2002; Yan et al., 2010; Yan and McKee, 2013; Krishnan et al., 2014). Second, *Drosophila* lacks a Rec8 orthologue. A related α-kleisin, C(2)M, and the mitotic Rad21 do not appear to have this role even though both appear on chromatin at the time of pre-meiotic S-phase, associate with cohesin components and are implicated in synaptonemal complex assembly or maintenance (Heidmann et al., 2004; Manheim and McKim, 2003; Urban et al., 2014). The absence of an identified α-kleisin for meiotic cohesion further raises the question of whether the α-kleisin-specific protease, Separase and its inhibitor, Pim have a role in *Drosophila* meiosis. Here, we determine the roles of these cohesion regulators by following chromosome behaviour in meiosis following genetic manipulation of Pim, Separase and cohesin components.

RESULTS

FISH probes against centromere-proximal and arm regions of the X-chromosome permit the monitoring of cohesion release in meiosis and in polar bodies

To follow chromosome behaviour in meiosis, we combined immunofluorescence, to detect microtubules, and fluorescence *in situ* hybridization (FISH), to visualize a single chromosome. We used two FISH probes, one against the 359-base peri-centromeric repeat on the X-chromosome (X-cent FISH probe) and one directed against a distal arm sequence on the X-chromosome (X-arm FISH probe). The description of wild-type meiosis below and in Fig. 4, is consistent with previous studies (e.g. Endow and Komma, 1997; Page and Orr-Weaver, 1997), and our use of arm and centromeric FISH probes provides a further degree of resolution. We first used these probes on eggs collected over a 2-h period. Meiosis is completed within 20 min of egg laying (Foe et al., 1993), and therefore most of these eggs have completed meiosis. At the completion of meiosis, the meiotic spindles disassembled and nuclei formed around the decondensed chromatin of the four meiotic products (Fig. 1A). In post-meiotic interphase, each nucleus had a single X-cent signal. The X-arm signal was detected in most of these nuclei, although it was sometimes diffuse or undetectable in interphase nuclei (arrowhead in Fig. 1A). If the egg is fertilized, one of these nuclei moved towards the male pronucleus, guided by the sperm-derived microtubule aster (Fig. 1A, arrow). The three remaining female pronuclei then underwent nuclear envelope breakdown, and microtubules reorganized to form the polar body

Department of Biological Sciences, University of Windsor, Windsor, Ontario, Canada N9B 2P1.
*Present address: Jordan University of Science and Technology, Irbid, Jordan.

‡Author for correspondence (aswan@uwindsor.ca)

Received 19 August 2015; Accepted 8 December 2015

Journal of Cell Science (2016) 129, 531-542 doi:10.1242/jcs.179358

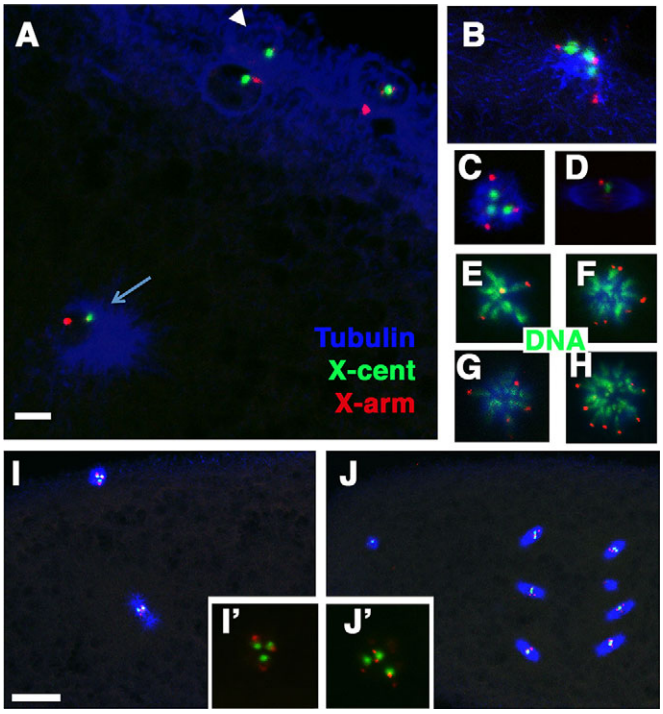

Fig. 1. Polar body formation and syncytial mitotic divisions in wild-type. (A–D) Wild-type embryos labelled for Tubulin, X-cent and X-arm FISH probes. (A) Wild-type fertilized egg in post-meiotic interphase. Male and female pronuclei are at the bottom left (arrow). The male pronucleus, which is largely obscured by its microtubule aster, is Y-bearing as it is not recognized by the FISH probes. Two of the three polar body nuclei have X-arm and X-cent FISH signal. The other does not have detectable X-arm FISH signal (arrowhead near top). (B) Polar body formation. The three polar body nuclei have undergone nuclear envelope breakdown and microtubules appear in the process of organizing around the chromatin. (C) Polar body with three X-chromosomes organized with centromeres near the centre and arms extending outward. (D) Metaphase of the first zygotic mitosis. Single X-cent and X-arm foci indicate this is a male XY embryo. (E,F) Polar bodies from fertilized eggs with three and six X-arms, respectively. (G,H) Polar bodies from unfertilized eggs, with four and eight X-arms, respectively. (I) Embryo in the first mitosis. Its polar body has three X-cent and three X-arm FISH dots (I′). (J) Embryo in cycle 3. Its polar body has three X-cent and five X-arm FISH dots (J′). Scale bars: 5 µm (A, images in B–H,I′,J′ are also shown at this scale); 20 µm (I, the image in J is also shown at this scale).

near the egg cortex (Fig. 1B). The polar body (Fig. 1C), which formed in concert with assembly of the first mitotic spindle of the zygote (Fig. 1D), is organized as a central microtubule array with chromosome arms radiating outwards (Foe et al., 1993). The X-cent FISH probe recognized three signals in the polar body, corresponding to the three haploid nuclei that join to form this structure (Fig. 1C,I,J, and see Fig. 7B,K). The X-arm probe, in contrast, recognized a variable number of foci, between three and six (Fig. 1C,E,F, Fig. 2A and see Fig. 7B,K). Based on cytological observations, it has been suggested that polar body chromosomes lose arm cohesion over time (presumably having replicated in the post-meiotic interphase) (Foe and Alberts, 1983). Indeed, we find that wild-type embryos prior to cycle three typically have three X-arm FISH signals, whereas later embryos have up to six (Figs 1I,J and 2A).

To determine whether the loss of arm cohesion on polar body chromosomes is dependent on fertilization or progression through mitotic cycles, we performed FISH on wild-type unfertilized eggs. Polar bodies from unfertilized eggs contain all four meiotic products (Foe and Alberts, 1983). If arm cohesion persists in these non-developing eggs, we would expect to see only four X-arm FISH signals per polar body. However, we found that unfertilized eggs had between four and eight X-arm FISH signals (Fig. 1G,H). Therefore, the loss of cohesion on polar body chromosome arms appears to occur as a function of time and is not dependent on fertilization or subsequent embryonic mitosis.

Non-degradable Pim in the female germline

Given that no α-kleisin has been identified for *Drosophila* meiosis, we considered the possibility that the machinery that controls α-kleisin cleavage, Separase and Securin, might not be involved in cohesion release in this system. To directly test whether Securin (Pim) destruction is necessary for the release of cohesion in female meiosis, we generated *pUASp* transgenes to allow germline-directed expression of wild-type (GFP–Pim^{wt}) or stabilized forms of Pim that lack the D-box (GFP–Pim^{d}) or both D-box and KEN-box (GFP–Pim^{dk}), based on equivalent *UASt-pim-myc* transgenes (*pim-myc*, *pim^{dba}-myc* and *pim^{kenadba}-myc*, respectively) (Leismann et al., 2000; Leismann and Lehner, 2003). We expressed these in the female germline using the maternal *α-Tubulin-Gal4-VP16* (*mat-Gal4*) driver. Western blotting revealed that GFP–Pim^{wt}, GFP–Pim^{d} and GFP–Pim^{dk} were expressed at levels comparable to endogenous Pim (Fig. S1A). Preliminary results revealed that GFP–Pim^{d} and GFP–Pim^{dk} produce identical phenotypes in the female germline (data not shown) so we chose GFP–Pim^{dk} for subsequent experiments.

To determine whether these *GFP-pim* transgenes retain Pim function, we first attempted to rescue a *pim* mutant with *GFP-Pim^{wt}*. However, the expression of *GFP-Pim^{wt}* using the Gal4 system resulted in lethality, both in a *pim* mutant and in a wild-type background (data not shown). Similar findings have been reported for *UASt-pim-myc*, apparently due to Pim overexpression resulting from use of Gal4 (Leismann et al., 2000). Despite the failure of rescue experiments, several other findings demonstrate that our *GFP-Pim* transgenes retain Pim function. First, co-immunoprecipitation experiments confirm that these proteins are able to bind to Separase *in vivo* (Fig. S1B). Second, we found that an untagged, stabilized *pim* transgene, *pUASp-Pim^{dk}* (*Pim^{dk}*), had identical phenotypes to *pUASp-GFP-Pim^{dk}* (see Fig. 2, Fig. S2), indicating that the GFP tag does not disrupt activity. Finally, as we show later, expression of stabilized Pim caused phenotypes that were essentially identical to those seen with loss of *Sse* (see Figs 4 and 5).

Pim destruction is necessary for the release of arm cohesion on polar body chromosomes

To determine whether meiosis was affected by stabilized Pim, we first examined embryos labelled for Tubulin and the X-cent FISH probe. In 0–2 h egg collections from fertilized wild-type females, almost all had completed meiosis and contained a single (or rarely two) polar bodies (96%, n=44). Almost all polar bodies (90%) contained three X-cent FISH dots, and thus three X-chromosomes (Fig. S2A,A′). Eggs from females expressing *GFP-Pim^{dk}* failed to hatch, but the majority appeared to complete meiosis, as indicated by the presence of a polar body in 89% of eggs (n=66). As in wild-type, the polar body contained three X-cent FISH signals (88% of all polar bodies) (Fig. S2B,B′), suggesting that one of the female pronuclei contributes to zygote formation. However, zygotic development was arrested early, and most embryos contained only one or two zygotic nuclei that ranged in appearance from normal to highly aberrant. Aberrant spindles typically appeared to contain excess chromatin and FISH signal, suggestive of re-replication (Fig. S2B).

Journal of Cell Science (2016) 129, 531-542 doi:10.1242/jcs.179358

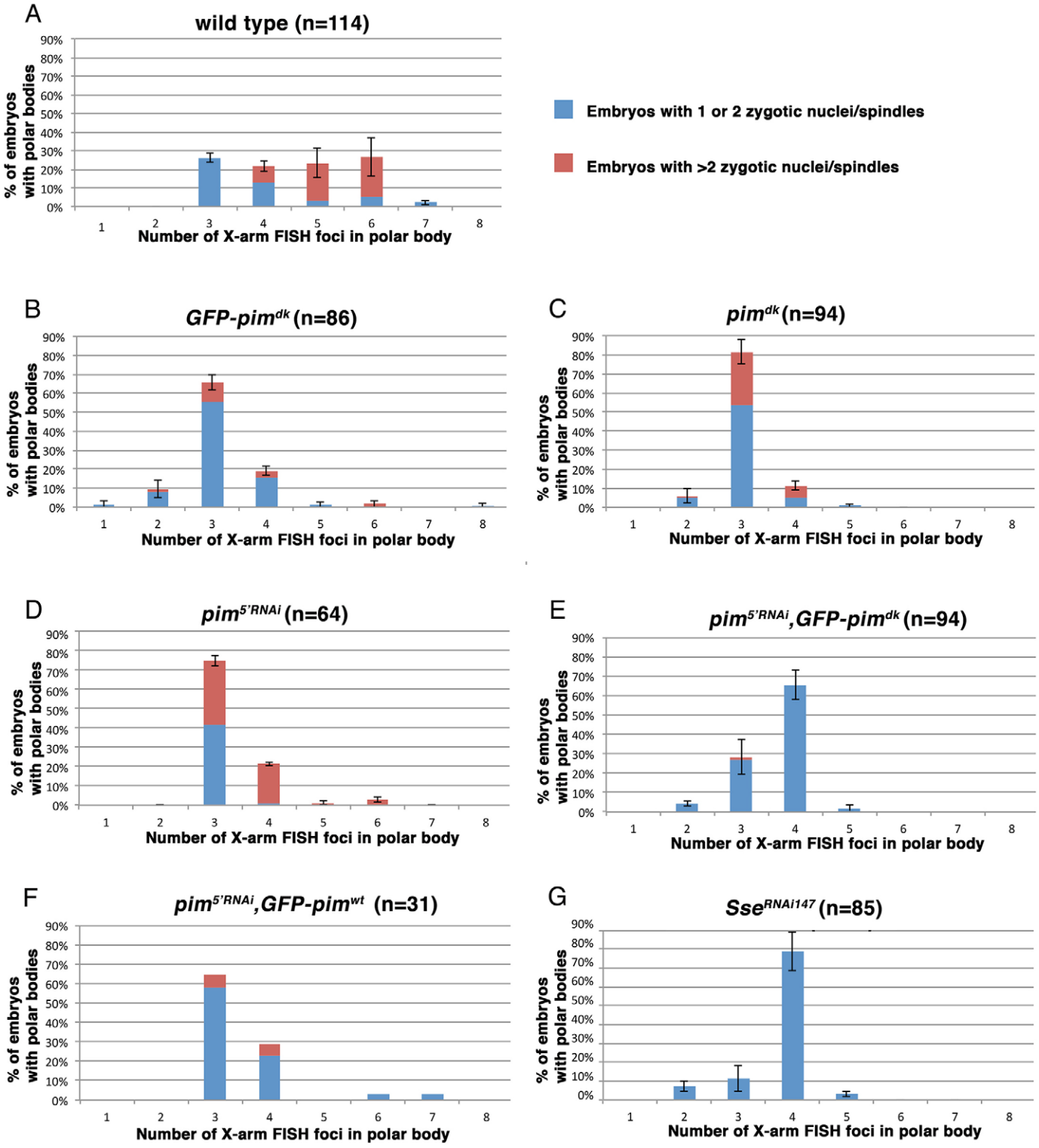

Fig. 2. Arm segregation in polar body chromosomes. 0–1 h embryos from wild-type females (A) or females expressing stabilized Pim (B,C), RNAi against *pim* (D) or *Sse* (G), or RNAi against *pim* with wild-type (F) or stabilized Pim (E), in all cases under the control of *mat-Gal4*. Embryos (*n* values are shown on the figure) were scored for number of X-arm FISH signals in their polar bodies and for mitotic stage. Panel F represents a single experiment. All other panels represent the combined results of three experiments and the error bars indicate s.e.m.

We also examined *GFP-Pim*^{dk} embryos using the X-arm FISH probe. As described above, wild-type embryos have up to six X-arm FISH signals in their polar bodies, depending on their age. *GFP-Pim*^{dk} embryos, in contrast, almost always had three (Fig. S2C; Fig. 2B). Given that wild-type polar body chromosomes normally lost arm cohesion even in unfertilized eggs (Fig. 1H), the apparent failure to release arm cohesion in *GFP-Pim*^{dk} polar bodies is likely not due to failure of embryonic development.

Journal of Cell Science (2016) 129, 531-542 doi:10.1242/jcs.179358

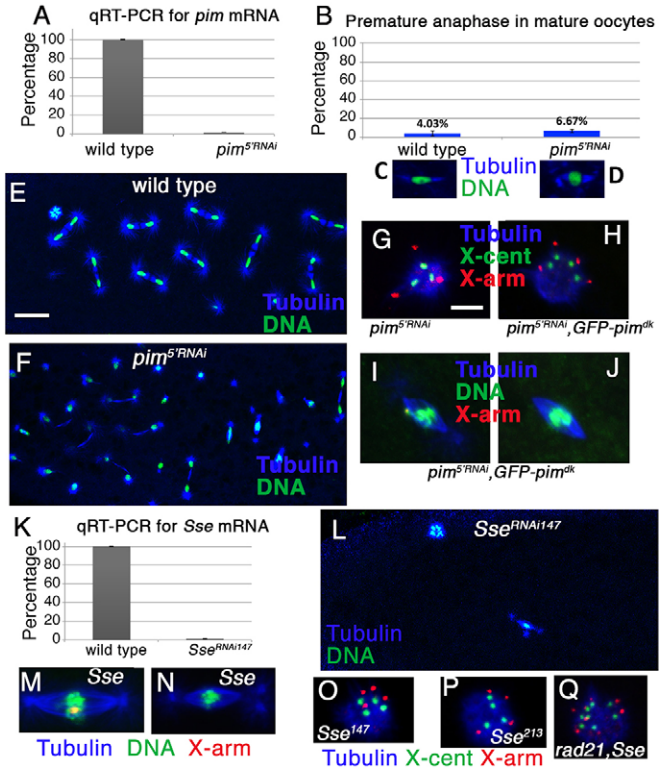

Fig. 3. *Pim* and *Sse* are required maternally for embryonic development and release of cohesion in polar body and syncytial nuclei. (A) qRT-PCR for *pim* mRNA in $pim^{5'RNAi}$ late-stage-enriched oocytes, showing the mean± s.e.m. (n=2, each with three repeats). *pim* levels in $pim^{5'RNAi}$ were 1.7%±0.2 of wild type. (B) Frequency of precocious chromosome segregation in stage 14 oocytes from wild-type and $pim^{5'RNAi}$ (n=67 for *yw* and n=60 for $pim^{5'RNAi}$). (C,D) Metaphase I arrest in stage 14 oocytes from wild-type (C) and $pim^{5'RNAi}$ (D). (E,F) Wild-type and $pim^{5'RNAi}$ embryos. The Pim-depleted embryo displays aberrant mitotic figures that are not synchronous. (G) Polar body from a $pim^{5'RNAi}$ embryo with three X-cent and three X-arm FISH dots. (H) Polar body from a $pim^{5'RNAi}$,$GFP\text{-}pim^{dk}$ embryo with four X-cent and four X-arm FISH dots. (I,J) Zygotic nuclei from two different $pim^{5'RNAi}$,$GFP\text{-}pim^{dk}$ embryos. The embyo in I has a single X-arm FISH dot and is thus haploid XO, whereas the embryo in J has no X-arm FISH signal and is thus YO. (K) qRT-PCR for *Sse* mRNA in late-stage-enriched $Sse^{RNAi147}$ oocytes (n=3, each with three repeats). *Sse* levels in $Sse^{RNAi147}$ were 1.2%±0.3 of wild type. (L) $Sse^{RNAi147}$ embryo arrested in the first mitotic division. (M,N) Mitotic spindles from two different $Sse^{RNAi147}$ embryos. The embryo in M has a single X-arm signal and is thus XO, whereas that shown in N has no X-arm signal and is thus YO. (O,P) Polar bodies from 0–1 h $Sse^{RNAi147}$ and $Sse^{RNAi213}$ embryos, respectively. In both embryos, the polar body has four X-cent and four X-arm FISH signals. (Q) Polar body from a $Rad21^{GL522}$, $Sse^{RNAi147}$ embryo with eight X-cent and eight X-arm FISH dots. Scale bars: 20 µm (E, and images in F,L are also shown at this scale); 5 µm (G and applies to all other images).

Importantly, untagged transgenic pim^{dk} gave an identical phenotype with respect to arm cohesion in polar bodies and arrest in early embryogenesis (Fig. S2C–H, Fig. 2C). Therefore the GFP tag does not contribute to these phenotypes. We conclude that the overexpression of stabilized Pim does not block the completion of meiosis but results in a failure to release cohesion on the arms of the polar bodies and produces an early arrest in the syncytial cycles.

Pim has dual roles in regulation of polar body chromosome segregation

In the above experiments, stabilized Pim was expressed in the presence of endogenous Pim. If, as in mitotic cells, Pim functions to bind and inhibit Separase, endogenous Pim would compete with transgenic non-degradable Pim for Separase binding. This endogenous Pim would be subject to degradation at anaphase, and therefore some Separase would be released that could allow progression through meiosis. To address this possibility, we sought to express $GFP\text{-}pim^{dk}$ in a background depleted of endogenous Pim. To achieve this, we generated a *UASp-pim* short hairpin RNA (shRNA construct; $pim^{5'RNAi}$) that specifically targets the 5′UTR of *pim* while not affecting *pim* transgenes (which lack native UTR sequences) (Fig. 3A). Before putting stabilized Pim in this background, we examined the effect of $pim^{5'RNAi}$ alone. Although the loss of *pim* might be expected to result in precocious activation of Separase, it has previously been found that zygotic loss of *pim* in fact gives a phenotype similar to that of stabilized Pim or loss of *Sse* (Stratmann and Lehner, 1996). Our results are consistent with such a dual role for Pim. First, examination of stage 14 oocytes by DNA staining (combined in some cases with Tubulin staining) revealed that $pim^{5'RNAi}$ oocytes did not undergo premature chromosome segregation (Fig. 3B–D). Second, $pim^{5'RNAi}$ eggs appeared to complete meiosis and make a polar body in which chromosome arms failed to lose cohesion over time (Figs 2D and 3G), like $GFP\text{-}pim^{dk}$. $Pim^{5'RNAi}$ embryos also displayed mitotic defects, although these were milder than those seen with $GFP\text{-}pim^{dk}$ (Figs 2D and 3F). Overall, the similarity between $pim^{5'RNAi}$ and $GFP\text{-}pim^{dk}$ phenotypes supports the idea that Pim has both positive and negative roles in controlling Separase (Stratmann and Lehner, 1996), and further supports our conclusion that the phenotypes observed with $pim^{5'RNAi}$ and $GFP\text{-}pim^{dk}$ are specific.

Our primary reason for generating $pim^{5'RNAi}$ was to permit the expression of non-degradable Pim in a background depleted of endogenous Pim. We therefore examined 0–1 h embryos from females that co-expressed both $pim^{5'RNAi}$ and $GFP\text{-}pim^{dk}$, and probed for Tubulin, X-cent and X-arm. Unlike $pim^{5'RNAi}$ alone or $GFP\text{-}pim^{dk}$ alone, both of which permitted some embryonic development (Fig. 2B,D), $pim^{5'RNAi}$,$GFP\text{-}pim^{dk}$ embryos arrested in the first or rarely, the second mitotic division (Fig. 2E). In addition, in contrast to $pim^{5'RNAi}$ or $GFP\text{-}pim^{dk}$ alone, there was no female contribution to zygote formation: in 50% of $pim^{5'RNAi}$, $GFP\text{-}pim^{dk}$ embryos (25/50) the lone mitotic spindle had a single X-cent FISH signal (Fig. 3I), and in 50% the mitotic spindle had no associated X-cent FISH signal (Fig. 3J). This indicates that the embryo forms solely from the male pronucleus (and therefore has either a single X or Y chromosome). The presence of a single X-cent and a single X-arm signal in the mitotic spindle (Fig. 3I) implies that cohesion is maintained along these mitotic chromosomes. Therefore stabilized Pim blocks cohesion release in the syncytial mitotic divisions as well as on polar body chromosomes.

The majority of 0–1 h $pim^{5'RNAi}$, $GFP\text{-}pim^{dk}$ embryos contained polar bodies (72%, n=129). These typically contained four X-arm and four X-cent FISH signals (Figs 2E and 3H), in contrast to the three X-arm and three X-cent FISH signals seen when $GFP\text{-}pim^{dk}$ was expressed in the pim^{+} background (Fig. 2B). The presence of four X-chromosomes is consistent with the absence of a female contribution to zygote formation, as described above. This apparent failure of zygote formation might in turn be a consequence of defects in meiosis, as we address below. In addition, the presence of four, rather than up to eight X-arm FISH signals in polar bodies from $pim^{5'RNAi}$, $GFP\text{-}pim^{dk}$ embryos indicates that polar body chromosomes fail to lose arm cohesion, as was seen in $pim^{5'RNAi}$ and $GFP\text{-}pim^{dk}$.

We also expressed the wild-type *GFP-pim* transgene in the $pim^{5'RNAi}$ background. Embryos of the $pim^{5'RNAi}$, $GFP\text{-}pim^{wt}$

Journal of Cell Science (2016) 129, 531-542 doi:10.1242/jcs.179358

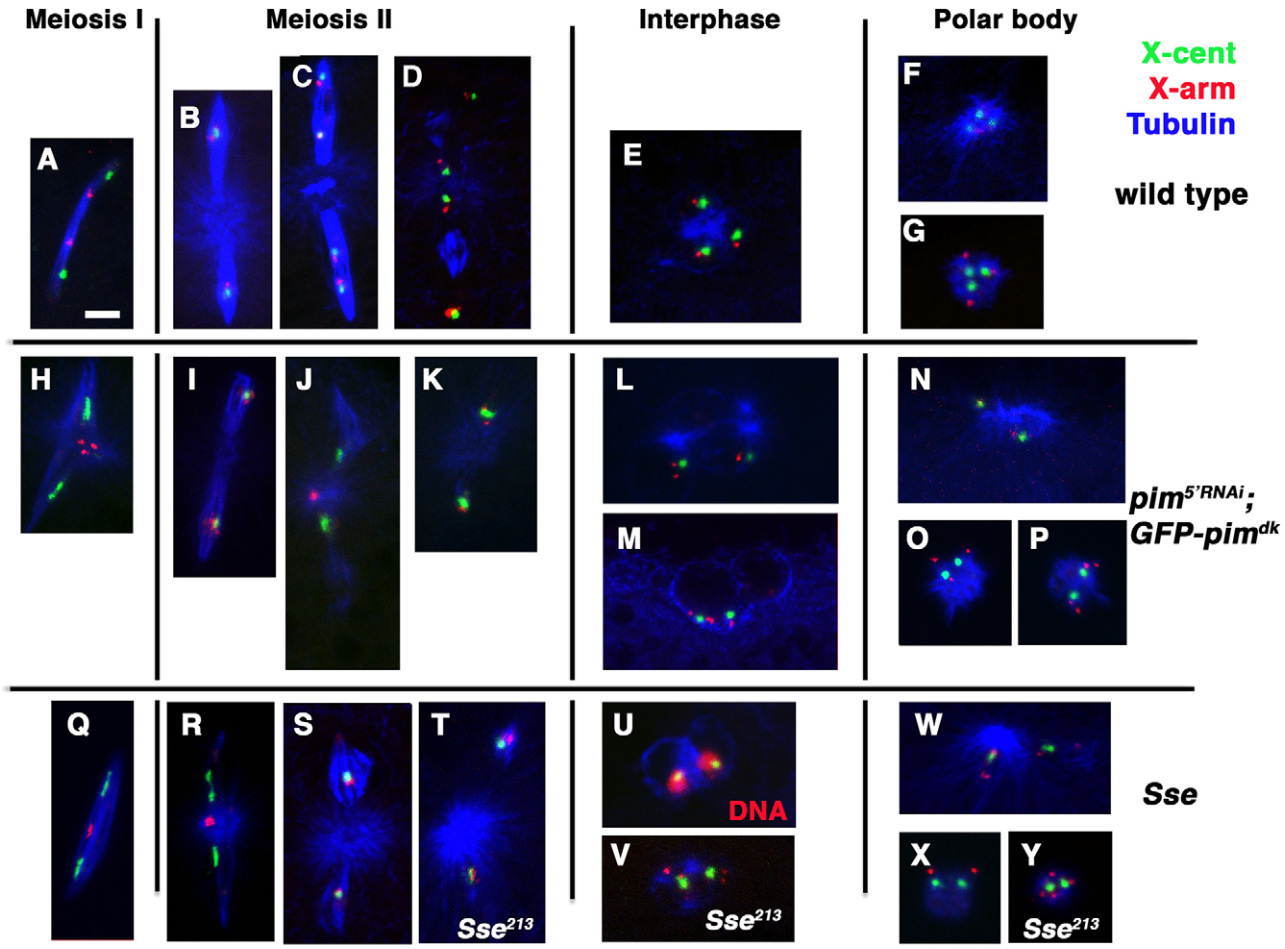

Fig. 4. Pim destruction and Sse activity are required for cohesion release in *Drosophila* meiosis. (A–H) Meiosis in wild-type oocytes. (A) Anaphase I showing separated X-cent and trailing arms. Scale bar: 5 µm. (B) Metaphase II with two X-cent signals. Arms are resolved on the upper spindle. (C) Early anaphase II with two X-cent and X-arm signals per spindle. (D) Later anaphase showing spindle disassembly. (E) Post-meiotic interphase (only the three cortical nuclei are shown). (F) Polar body assembly. (G) Polar body. (H–P) Meiosis in $pim^{5'RNAi}$,*GFP-*pim^{dk} oocytes. (H) Anaphase I with X-arms lagging at the spindle midzone. X-cent signal appears stretched and spindle morphology is aberrant. (I) Normal-appearing metaphase II. (J) Metaphase II with arms remaining at the central aster. (K) Oocyte in which the meiotic spindle appears to be disassembling (similar to the anaphase II in D), but still retaining centromeric cohesion. (L) Post-meiotic interphase. X-cent cohesion persists in both, and arm cohesion persists in one of the two nuclei. (M) Post-meiotic interphase in which the two X-homologues are within a single nucleus. (N) Polar body assembly. Centromeric and arm cohesion persists. (O) Polar body in which centromeric and arm cohesion persists. (P) Polar body in which centromeric but not arm cohesion persists. (Q–Y) Meiosis in *Sse* oocytes. All oocytes are $Sse^{RNAi147}$ except T,V and Y, which are $Sse^{RNAi213}$. (Q) Anaphase I in which arms failed to separate. (R) Metaphase II in which X-arms failed to separate. One of the X-centromeres appears highly stretched. (S) Normal-appearing metaphase II. (T) Metaphase II with spindle morphology similar to anaphase II. (U) Post-meiotic interphase (labelled for DNA, X-cent and Tubulin) in which centromeric cohesion persists. All chromatin is within two post-meiotic nuclei. (V,W) Post-meiotic interphase and polar body formation, respectively, in which X-cent cohesion persists while arm cohesion has released. (X,Y) Polar bodies with X-cent cohesion. In X, arm cohesion also persists.

genotype resembled those of $pim^{5'RNAi}$ or *GFP-*pim^{dk} alone (Fig. 2F). The weaker phenotype compared to $pim^{5'RNAi}$, *GFP-*pim^{dk} is consistent with the idea that the strong phenotype seen in $pim^{5'RNAi}$,*GFP-*pim^{dk} is due to the combined effect of Pim overexpression and stabilization.

Securin destruction is necessary for timely release of arm cohesion in meiosis I and centromere-proximal cohesion in meiosis II

To determine whether the overexpression of stabilized Pim in a background depleted of endogenous Pim disrupts meiosis, we examined oocytes that were actively undergoing meiosis at the time they were fixed. These were obtained from 20-min egg-lays and from *in vitro* activation of oocytes. Eggs were labelled for Tubulin, X-cent and X-arm. Eggs were then categorized according to meiotic stage, as determined by spindle or microtubule organization, and assessed for the presence or absence of centromere cohesion and arm cohesion. Representative images are shown in Fig. 4 and quantified in Fig. 5. We first examined meiosis in wild-type eggs. The metaphase I arrest was broken at ovulation, or experimentally, by *in vitro* activation. Anaphase I is characterized by elongation of the meiotic spindle and separation of the X-cent FISH signals (Fig. 4A). The separation of homologues at anaphase I requires the loss of cohesion distal to the chiasma, and therefore we expected to see four distinct X-arm FISH signals from this stage onwards. However, in most cases, we observed only two X-arm signals in anaphase I, indicating that arms remain closely apposed at this stage (Fig. 4A). Loss of arm cohesion could be inferred nonetheless by the separation of the two X-arm foci as the chromosomes are pulled to either spindle pole (Fig. 4A). Metaphase II is characterized by assembly of two tandem spindles with a central microtubule aster between them (Riparbelli and Callaini, 1996). Both spindles had a single X-cent signal (Fig. 4B). Sister chromatid arms could be distinguished in some cases, as seen for one of the two spindles in

Journal of Cell Science (2016) 129, 531-542 doi:10.1242/jcs.179358

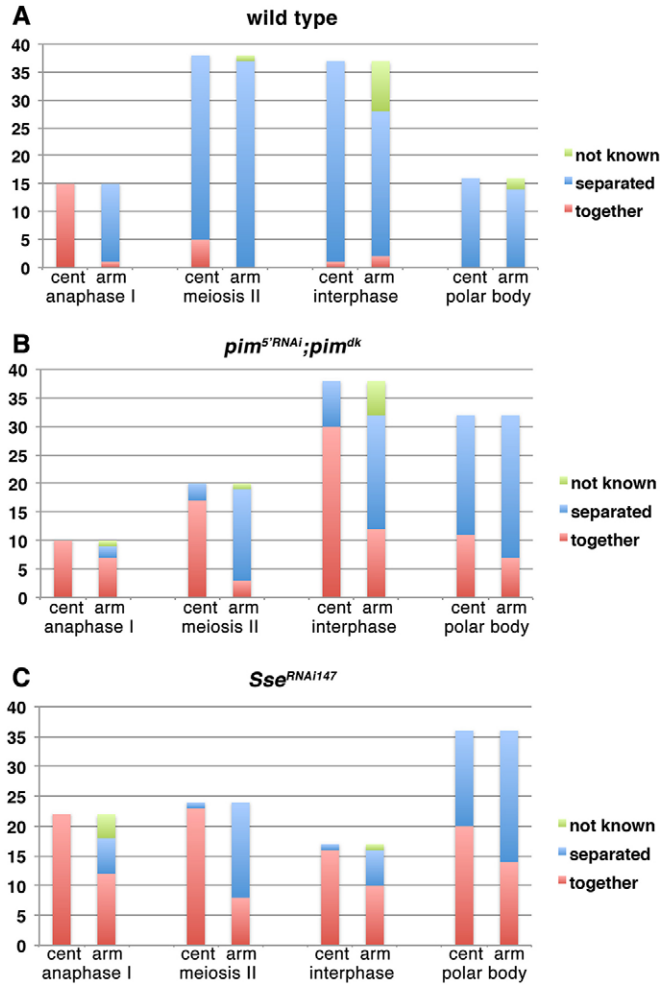

Fig. 5. Delayed release of arm and centromeric cohesion upon stabilization of Pim or knockdown of *Sse*. Frequency of meiotic phases and status of centromeric and arm cohesion in wild-type (A), *pim*$^{5′RNAi}$,*GFP-pim*^{dk} (B) and *Sse*^{RNAi147} oocytes (C). Eggs were obtained from *in vitro* activation or short (0–20 min) egg collections and were classified according to stage of meiosis (based on spindle or microtubule morphology). The data represents combined results for two *in vitro* activation and four 20-min egg collection experiments for each genotype. For anaphase I and meiosis II oocytes, arm cohesion is assumed to be present if the arms remain at the meiosis I spindle midzone (or central aster in the case of meiosis II). For later stages, arm cohesion is scored as present if there is one X-arm signal per X-cent. For all meiotic stages, centromere-proximal cohesion is scored as present if only two X-cent signals are detected. Eggs in which a polar body appears to be in the process of being formed (such as those shown in Fig. 4F,N,W) were grouped with eggs in post-meiotic interphase. The number of X-arm signals could not be reliably scored in some post-meiotic interphase oocytes and in a small number of oocytes of other stages. These were classified as not known.

Fig. 4B. Anaphase II separation of sister chromatids initiates with the release of centromeric cohesion. This was marked by the appearance of two X-cent signals per spindle (Fig. 4C,D). Sister chromatid arms also appeared to separate in anaphase II (Fig. 4C,D). In late anaphase II, the spindle changes morphology as it begins to disassemble (Riparbelli and Callaini, 1996) (Fig. 4D). Post-meiotic interphase (Fig. 4E), polar body formation (Fig. 4F) and the mature polar body (Fig. 4G) were described earlier (Fig. 1), and are shown again here for comparison to the findings described below.

We next examined meiosis in *in vitro*-activated and 0–20 min eggs of genotype *pim*$^{5′RNAi}$,*GFP-pim*^{dk}. The relative frequencies of the different meiotic stages (using spindle morphology and microtubule organization to determine stages) were similar between wild-type and *pim*$^{5′RNAi}$,*GFP-pim*^{dk} (Fig. 5A,B), suggesting that the stabilization of Pim does not result in an arrest or delay at any specific meiotic stage. However, as we describe below, cohesion release and consequent chromosome movements in meiosis were delayed. In *pim*$^{5′RNAi}$,*GFP-pim*^{dk} eggs that are in anaphase I, the arms often appeared to lag at the spindle midzone, even as centromeres were moving towards the poles (Fig. 4H). This apparent failure of arm release was seen in seven of ten *pim*$^{5′RNAi}$,*GFP-pim*^{dk} anaphase I oocytes compared to one of 15 for wild type (Fig. 5A,B).

Of 38 eggs from wild-type females that were in meiosis II, only five (13%) were in metaphase, as indicated by presence of a single X-cent FISH signal per spindle (Figs 4B and 5A). All others had lost centromeric cohesion and therefore were in anaphase II (Figs 4C,D and 5A). In *pim*$^{5′RNAi}$,*GFP-pim*^{dk} oocytes, we found the opposite ratio: 85% (17/20) of oocytes in meiosis II had a single X-cent FISH signal per spindle, and thus appeared to be in metaphase II (Figs 4I,J, K and 5B). Often the spindles appeared to be in the process of disassembly as if in the late stages of anaphase II (Fig. 4K, compare to 4D). These findings suggest that centromeric cohesion does not release properly in *pim*$^{5′RNAi}$,*GFP-pim*^{dk} eggs.

A total of 15% (3/20) of *pim*$^{5′RNAi}$,*GFP-pim*^{dk} eggs that we identified as being in meiosis II had X-arms associated with the central aster between the two spindles, a site that corresponds to their original location in metaphase I (Figs 4J and 5B). This phenotype, which was never observed in wild type (n=38) (Fig. 5A), appears to represent a failure of arm release in oocytes that have otherwise progressed into the second meiotic division. As described below, in *pim*$^{5′RNAi}$,*GFP-pim*^{dk} eggs, arm cohesion could also persist beyond the completion of meiosis.

Wild-type eggs in post-meiotic interphase had three cortical nuclei (plus male and female pronuclei in the egg interior), and in 97% (36/37) of these, each nucleus contained a single X-cent FISH signal (Figs 1A, 4E and 5A). In *pim*$^{5′RNAi}$,*GFP-pim*^{dk} eggs that are in post-meioitic interphase, only 21% (8/38) had this pattern. The remaining 79% of oocytes displayed a phenotype that we never saw in wild type: they either had only two cortical nuclei, both with a single X-cent FISH signal (Fig. 4L) or rarely, had two nuclei, one of which had both X-cent foci (Fig. 4M). In both cases, the two FISH signals appeared to represent the two sister chromatid pairs that failed to segregate at anaphase II. Therefore in the majority (79%) of *pim*$^{5′RNAi}$,*GFP-pim*^{dk} eggs, centromeric cohesion persisted into the post-meiotic interphase (Fig. 5B). Arm cohesion also persisted in 38% of these post-meiotic oocytes, as indicated by the presence of less than four X-arm signals (Figs 4L and 5B). Presumably in these cases, chiasma are not resolved and chromatin is either stretched between the two nuclei or broken.

In *pim*$^{5′RNAi}$,*GFP-pim*^{dk} eggs, the two nuclei generated upon completion of meiosis underwent nuclear envelope breakdown and assembled into polar bodies that resembled wild-type polar bodies. However, in *pim*$^{5′RNAi}$,*GFP-pim*^{dk} eggs obtained from 0–20 min collections, centromeric cohesion persisted in 34% (11/32) and arm cohesion persisted in 22% of polar bodies (Figs 4O,P and 5B). As described above, polar bodies seemed to eventually arrest with four distinct X-cent and X-arm FISH foci (Figs 2F and 3H). We conclude that the overexpression of stabilized Pim results in a delay in the release of both arm cohesion and centromeric cohesion in meiosis.

Separase is required for release of cohesion in meiosis and in polar bodies

The results presented so far indicate a role for Securin destruction in meiosis and lead us to predict that Separase is also required in

Journal of Cell Science (2016) 129, 531-542 doi:10.1242/jcs.179358

Drosophila meiosis. To directly test this, we generated two non-overlapping RNAi lines that target *Separase* (*Sse*). Upon expression in the female germline under *mat-GAL4*, $Sse^{RNAi147}$ and $Sse^{RNAi213}$ both resulted in complete sterility. $Sse^{RNAi147}$ (Fig. 3K) was chosen for most experiments, but all phenotypes were also seen with $Sse^{RNAi213}$ (see below). To determine the consequences of *Sse* knockdown, we first examined embryos from 0–1 h egg collections. *Sse* embryos invariably arrested with a single mitotic spindle (Figs 2G and 3L). In $Sse^{RNAi147}$, as in $pim^{5′RNAi}$,*GFP-pim*^{dk}, approximately half of all embryos (21/50) lacked an X-chromosome in the mitotic spindle (Fig. 3M,N), suggesting that zygote formation fails. Consistent with this conclusion, and again identical to $pim^{5′RNAi}$,*GFP-pim*^{dk}, the majority of embryos from $Sse^{RNAi147}$ and $Sse^{RNAi213}$ females contained polar bodies with four X-cent and X-arm signals (Figs 2G and 3O,P).

To determine whether Sse is required for cohesion release in meiosis we collected eggs from *in vitro*-activated oocytes and from 0–20 min egg collections, and analysed these as we did for $pim^{5′RNAi}$,*GFP-pim*^{dk}. The quantification in Fig. 5C and most images described below come from $Sse^{RNAi147}$, but the same phenotypes were seen in $Sse^{RNAi213}$ (Fig. 4T,V,Y). As with stabilized Pim, it appeared that there was no major delay in meiosis (again using microtubule organization to determine stages) (compare Fig. 5A and C). In *Sse*, arm cohesion persisted in anaphase I, and to a lesser extent, throughout meiosis (Figs 4Q,R,X and 5C). Centromeric cohesion also persisted, such that 96% (23/24) of $Sse^{RNAi147}$ oocytes in meiosis II were in metaphase II (based on presence of a single X-cent FISH signal per spindle) (Figs 4S and 5C). A similar failure of anaphase II was seen in $Sse^{RNAi213}$ (Fig. 4T). As with stabilized Pim, the failure of anaphase II results in the generation of two rather than four daughter nuclei at the completion of meiosis, and these two nuclei both had a single X-cent signal (Fig. 4U,V). The persistence of centromeric cohesion into the post-meiotic interphase was seen in 94% (16/17) of $Sse^{RNAi213}$ oocytes (Fig. 5C). The two meiotic products generated in *Sse* oocytes come together to form polar bodies that contained two X-cent FISH signals (Fig. 4W–Y). Of 36 embryos from $Sse^{RNAi213}$ that contained polar bodies, 56% appeared to have retained centromeric cohesion (Fig. 5C). We conclude that Separase is required for the timely release of arm cohesion in anaphase I and centromeric cohesion in anaphase II.

SMC3 is required for arm cohesion in meiosis

Separase brings about cohesion release by targeting the α-kleisin, Rad21 in mitosis, or Rec8 in meiosis. *Drosophila* lacks a meiotic α-kleisin and recent evidence argues against Rad21 serving this meiotic function (Urban et al., 2014). Specifically, it has been found that induced cleavage of a TEV-cleavable version of Rad21 does not lead to premature chromosome segregation, and a putative non-cleavable version of Rad21 could not prevent anaphase chromosome segregation (Urban et al., 2014). Meanwhile, recent genetic evidence, based on genetic segregation assays, has implicated the cohesin-loading factor, Eco, and the cohesin component, SMC1, in cohesion in meiosis (Weng et al., 2014). To complement these studies, we used our X-chromosome FISH probes to directly assess the effect of Rad21 and SMC3 depletion on cohesion in meiosis. We obtained shRNA transgenes directed against *Rad21* ($Rad21^{GL522}$) and *SMC3* ($SMC3^{GL518}$) (Ni et al., 2011). When expressed under the control of *mat-Gal4*, we observed efficient knockdown (Fig. 6A,B) and the production of eggs that failed to hatch (see below). We wanted to specifically knock down these genes before and during the pre-meiotic S-phase, when cohesion is established. Therefore, we turned to the *nos-Gal4* driver. This driver expresses throughout oogenesis at levels comparable to *mat-Gal4*, but it begins earlier, prior to the pre-meiotic S-phase (Sugimura and Lilly, 2006; Staller et al., 2013). We first examined mature stage 14 oocytes using a DNA dye and X-cent FISH probe. Wild-type stage 14 oocytes are arrested in metaphase I and had a single major DNA mass and two X-cent FISH foci oriented towards the spindle poles (Dernburg et al., 1996) (Fig. 6C,D), indicative of a stable metaphase I arrest. $Rad21^{GL522}$ oocytes are indistinguishable from wild type at this stage (Fig. 6C). In contrast, half of all $SMC3^{GL518}$ oocytes had more than one DNA mass (Fig. 6C,E). In most of these oocytes, the X-cent FISH signals appeared in distinct DNA masses (Fig. 6E). Therefore, SMC3 depletion leads to precocious homologue segregation. We never observed more than two X-cent FISH signals, indicating that sister chromatid cohesion along centromeres is maintained. Double knockdown of *SMC3* and *Rad21* did not significantly increase the frequency of this phenotype (Fig. 6C), supporting the conclusion that Rad21 has no role in meiotic cohesion.

The failure to maintain a stable metaphase I arrest in *SMC3* oocytes suggests a specific failure of arm cohesion. However, precocious homologue segregation can also result from a failure to establish chiasma. Cohesin subunits, SMC1 and SMC3, colocalize with synaptonemal complex components such as C(3)G during meiotic pachytene (Khetani and Bickel, 2007), and mutations in *SMC1* or knockdown of *SMC3* result in synaptonemal complex defects (Tanneti et al., 2011; Weng et al., 2014). In *Drosophila*, synaptonemal complex formation is required for chiasma formation. Therefore, the failure to maintain metaphase I arrest in *SMC3* oocytes could be due to a failure to undergo crossing over and may not be due to failed arm cohesion.

To directly assess arm cohesion in Rad21-depleted and SMC3-depleted oocytes, we employed the X-arm FISH probe. If arm cohesion is unaffected, we expect to see two distinct foci corresponding to the two homologues. If arm cohesion is disrupted, we expect to see up to four foci per oocyte. We first examined stage 14 oocytes, but were surprised to find that the X-arm FISH probe did not give specific signal in oocytes at this stage. Rather, it non-specifically labelled all chromatin (Fig. 6F,G). However, this probe gave specific signal throughout the post-pachytene stages of meiotic prophase (oogenesis stages 7 to 12). In 91% of wild-type oocytes in stages 9–11 of oogenesis, the X-arm FISH probe detected one or, more often, two foci in the oocyte nucleus (Fig. 6H,M). The remaining 9% of oocytes had three or four X-arm foci (Fig. 6M). This is consistent with previous findings (Dernburg et al., 1996; Hughes and Hawley, 2014). A similar pattern is observed in *Rad21* oocytes: 83% had either one or two X-arm foci (Fig. 6I,M). In contrast, 45% of *SMC3* oocytes had one or two X-arm foci, whereas 55% had three or four (Fig. 6J–M). In addition, the X-arm foci often appeared to be more diffuse than those seen in either wild type or *Rad21*. Of those *SMC3* oocytes with one or two distinct X-arm foci, almost half showed a diffuse staining pattern on at least one of the foci (Fig. 6L,M). These might represent situations in which arm cohesion is partially but not completely disrupted. The diffuse staining and, in particular, the occurrence of three or four X-arm foci is cytological evidence that SMC3 is required for arm cohesion in *Drosophila* meiosis.

SMC3 and Rad21 are required for cohesion in polar body chromosomes

To examine the requirements for SMC and Rad21 after meiosis, we knocked down these genes using *mat-Gal4*. With this driver, $Rad21^{GL522}$ and $SMC3^{GL518}$ embryos progress through syncytial

Journal of Cell Science (2016) 129, 531-542 doi:10.1242/jcs.179358

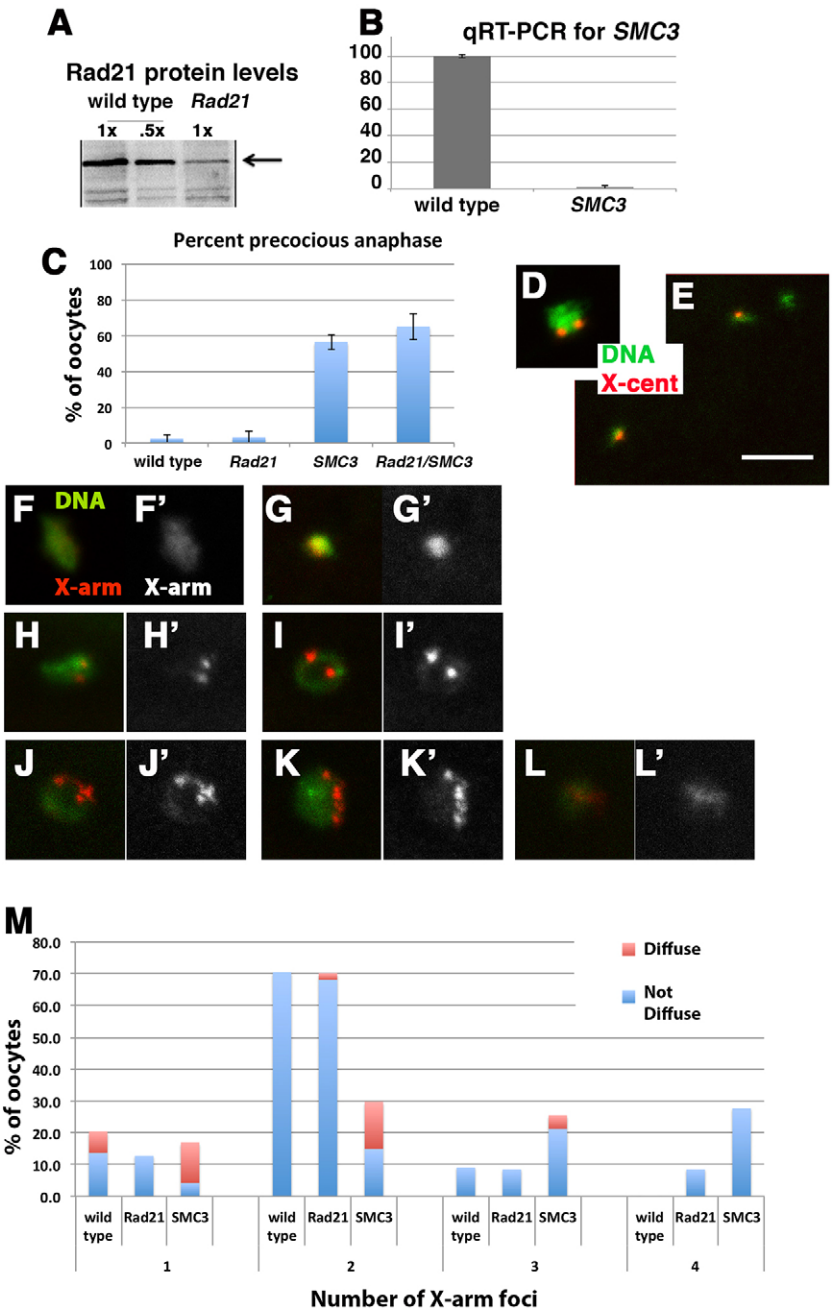

Fig. 6. SMC3 is required for arm cohesion in meiosis. (A) Representative western blot for Rad21 in late-stage-enriched oocytes (arrow indicates Rad21). Based on three independent experiments, Rad21 levels in *Rad21*^{GL522} are 16.8±2.3% (mean±s.e.m.) of wild type. (B) qRT-PCR results for *SMC3* mRNA in *SMC3*^{GL518} late-stage-enriched oocytes. Shown is the mean±s.e.m. result from three experiments (each with three repeats). *SMC3* mRNA levels in *SMC3*^{GL518} are 1.3%±0.4 of wild-type levels. (C) Frequency (mean±s.e.m.) of precocious chromosome segregation in stage 14 oocytes from wild-type, *Rad21*^{GL522}, *SMC3*^{GL518} and double knockdown, all with *nos-GAL4*. Results are from three independent experiments. (D,E) Stage 14 wild-type (D) and *SMC*^{GL518} (E) oocytes labelled for DNA and the X-cent FISH probe. Scale bar: 5 µm. (F,G) Wild-type and *SMC*^{GL518} stage 14 oocytes labelled for DNA and the X-arm FISH probe. (H–L) Stage 9–11 oocytes labelled for DNA and the X-arm FISH probe. (H,I) Wild-type and *Rad21*^{GL522} oocytes with two distinct X-arm foci in the oocyte nucleus. (J,K) *SMC*^{GL518} oocyte nuclei with three and four X-arm foci, respectively. (L) *SMC*^{GL518} oocyte nucleus with one diffuse X-arm focus. (M) Graph depicting percentage of oocytes with one, two, three or four X-arm FISH foci in oocyte nuclei as well as the percentage in which at least one of the FISH foci appears diffuse. A total of 44 wild-type, 47 *Rad21*^{GL522} and 47 *SMC*^{GL518} oocytes between stages 9–11 were examined.

divisions that become progressively aberrant and asynchronous (Fig. 7E,H, compare to A). Although the first few syncytial cycles appeared to be less disrupted, the FISH patterns were suggestive of precocious chromosome segregation (Fig. 7G,J, compare to C,D).

Rad21 and *SMC3* eggs appeared to complete meiosis, as indicated by the presence of a polar body (Fig. 7F,I, compare to B). It can also be inferred that one of the female meiotic products successfully joined the male pronucleus to form the zygote, based on the presence of at least one X-cent FISH signal in the zygotic nuclei of all embryos from *Rad21* and *SMC3* knockdowns (n>100 for both). If zygote formation had failed, half of these embryos (those fertilized by a Y-bearing sperm) would lack an X-chromosome in their embryonic nuclei.

As described above, in wild-type fertilized eggs, the polar body has three of each chromosome, and therefore three X-cent FISH signals (Figs 1 and 7B,K). In *Rad21* and *SMC3* embryos, the number of X-cent signals in the polar body was often greater than three, and most often, six X-cent signals were detected (Fig. 7F,I,L,M). This suggests that polar body chromosomes lack centromeric cohesion. The number of embryos with six X-arm FISH signals per polar body is also higher than in wild type, (Fig. 7K–M), suggesting that arm cohesion is also lost prematurely or is not established. We conclude that Rad21 and SMC3 are required for centromeric and arm cohesion on polar body chromosomes.

We argued earlier that the presence of four (as opposed to eight) X-arm signals per polar body in *pim*$^{5'RNAi}$,*GFP-pim*^{dk} and *Sse* knockdown eggs reflects failed release of arm cohesion on polar body chromosomes. Alternatively, it is possible that DNA replication does not occur in the post-meiotic interphase, perhaps as a consequence of aberrant meiosis. We generated *Rad21*, *Sse* double knockdown eggs to help distinguish between these possibilities. We expect that *Rad21*, *Sse* eggs would fail to

Journal of Cell Science (2016) 129, 531-542 doi:10.1242/jcs.179358

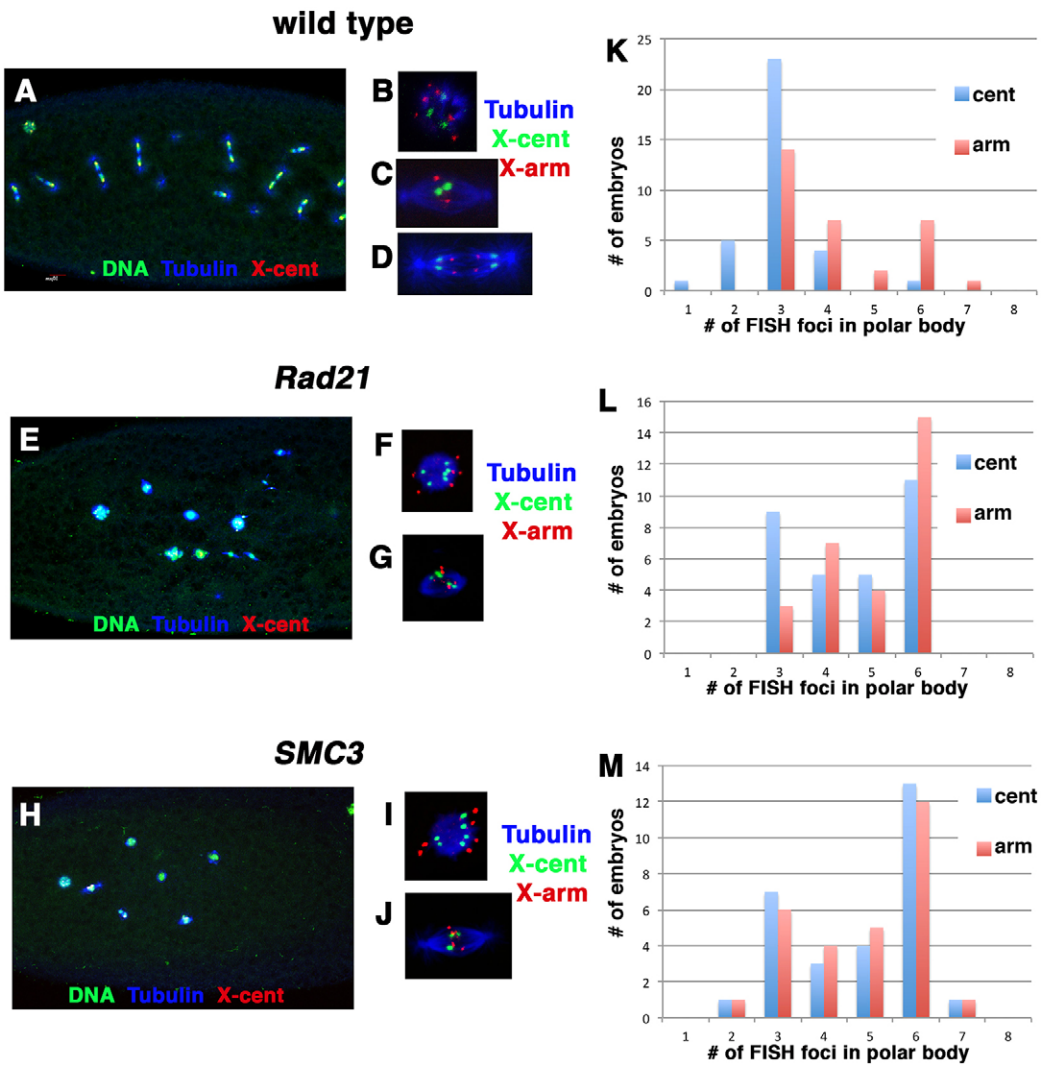

Fig. 7. Knockdown of *SMC3* and *Rad21* disrupts polar body formation and syncytial mitosis. (A–D) Images from four different wild-type embryos showing synchronized zygotic nuclei (A), polar body (B) and zygotic nuclei in metaphase (C) and anaphase (D). (E–G) *Rad21*^{GL522} embryos. (E) Whole embryo with non-synchronized, aberrant zygotic nuclei. (F) Polar body with six X-cent and six X-arm foci. (G) Mitotic spindle from an early stage *Rad21* embryo. The spindle appears to lack centrosomes, and X-cent and X-arm probes reveal separated sister chromatids. (H–J) *SMC3*^{GL518} embryos. (H) Whole embryo with non-synchronous aberrant zygotic nuclei. (I) Polar body with six X-cent and six X-arm foci. (J) Zygotic nucleus that appears to be in metaphase but with premature chromosome segregation. (K–M) Graphs showing number of X-cent and X-arm FISH foci in polar bodies from wild-type, *Rad21*^{GL522} and *SMC3*^{GL518} embryos. Graphs represent findings from three experiments with a total *n* of 34 for K, 30 for L and 29 for M.

complete meiosis and all four meiotic products would go into the polar body, as in *Sse* alone. If post-meiotic DNA replication fails, we would see four X-cent and X-arm signals. By contrast, if all four meiotic products replicated post-meiotically, but failed to establish cohesion (due to Rad21 depletion), polar bodies would contain up to eight X-cent and X-arm FISH signals. This is exactly what we see in the *Rad21*, *Sse* double knockdown (Fig. 3Q), supporting our conclusion that *Sse* (and presumably *pim*$^{5'RNAi}$,*GFP-pim*^{dk}) polar body chromosomes replicate but fail to release arm cohesion.

DISCUSSION

Separase activity and Securin destruction are necessary for female meiosis in *Drosophila*

In meiosis, sister chromatid cohesion is released in two steps: cohesion along chromosome arms distal to chiasma is released in anaphase I, whereas centromere-proximal cohesion is released in anaphase II (Watanabe, 2005). By expressing a stabilized form of Pim and by RNAi-mediated knockdown of *Sse*, we found that Securin destruction and Separase activity are required for both phases of cohesion release in *Drosophila* (Figs 4 and 5). The persistence of cohesion upon Pim stabilization or Sse depletion results in a failure to complete the second meiotic division, resulting in the production of two haploid but 2c nuclei at the completion of meiosis. This appears to be incompatible with successful zygote formation (Fig. 3).

Although the stabilization of Pim and knockdown of *Sse* result in a delay in the release of meiotic cohesion, this cohesion eventually releases, often after the completion of meiosis (Fig. 4). Thus, older embryos typically have polar bodies with four separated X-arm and X-cent FISH signals (Figs 2 and 3). There are many possible explanations for this gradual release of cohesion. First, knockdown of *pim* and *Sse* might not be complete. Although RNAi reduces their mRNA levels to 1–2% of endogenous levels, we do not know how much protein persists, and even if we knew this we would not know how much protein is sufficient to provide partial activity. We attempted to generate a stronger *Sse* knockdown by using the

Journal of Cell Science (2016) 129, 531-542 doi:10.1242/jcs.179358

nos-Gal4 driver, but this resulted in rudimentary ovaries, likely due to a requirement for Separase in the mitotic divisions that precede meiosis (A.S., unpublished). Although it is possible that residual Separase activity is responsible for the gradual release of cohesion in meiosis, we note that, in contrast to meiotic cohesion, the cohesion that is established post-meiotically is stable: in $pim^{5'RNAi}$, $GFP\text{-}pim^{dk}$ and *Sse*-knockdown embryos arm cohesion persists on polar body chromosomes (Fig. 2), and apparently also on mitotic chromosomes (Fig. 3). Another explanation for the gradual cohesion release is that a second pathway functions in parallel with Separase. In mitotic cells, the bulk of arm cohesion is released prior to anaphase through the Wapl-dependent prophase pathway (Peters and Nishiyama, 2012). It is possible that this or another Separase-independent pathway can contribute to cohesin removal in *Drosophila* meiosis.

We found that the overexpression of a stabilized version of Pim leads to a phenotype that is essentially indistinguishable from that seen upon *Sse* knockdown. This means that Pim is able to completely or near-completely inhibit Separase, but it does not imply that Pim is the only regulator of Separase in *Drosophila* meiosis. In mammals, Cdk1–Cyclin-B functions in parallel with Securin to keep Separase inactive prior to anaphase of meiosis I (Gorr et al., 2006), and the stabilization of Cyclin B1 inhibits sister chromatid disjunction (Herbert et al., 2003; Madgwick et al., 2004). In *Drosophila*, expression of Cyclin B with a mutant destruction box causes a meiosis arrest (Swan and Schupbach, 2007). Meanwhile, genetic evidence implicates Cyclin A as a regulator of Separase in mitotic cells (Leismann et al., 2000). It will be interesting to determine whether either or both cyclin and Cdks regulate Separase in *Drosophila* meiosis.

Sister chromatid cohesion in *Drosophila* female meiosis

We found that *SMC3* knockdown results in precocious segregation of X-chromosome homologues in ∼50% of stage 14 oocytes. In addition, roughly the same percentage of stage 9 to 11 *SMC3* oocytes appeared to have lost arm cohesion on the X-chromosome (Fig. 6). This is direct cytological evidence that SMC3 is required for cohesion in meiosis, and argues that the precocious homologue segregation observed in these oocytes is due, at least in part, to failed cohesion. Given the established role of cohesins in the synaptonemal complex, and thus in chiasma formation, it is also likely that some of the precocious homologue segregation we see is due to failed synapsis. Our results agree with a recent genetic study implicating SMC1 and the cohesin loader Eco in meiotic cohesion (Weng et al., 2014). This study found that partial knockdown of *Eco* or *SMC1* leads to meiotic non-disjunction events, even in cases where crossing over had occurred (Weng et al., 2014). Our results provide direct cytological evidence to support their findings. It is interesting to note that *SMC3* oocytes only appear to show cohesion defects on chromosome arms (Fig. 6). It is possible that residual SMC3 following RNAi knockdown is sufficient to keep centromeric regions together. Alternatively, it might mean that cohesion near the centromere does not depend solely on SMC3 and the canonical cohesin complex.

Although the cohesin complex appears to have a conserved role in *Drosophila* meiosis, the identity of the Separase target within this complex remains unknown. The Rec8-related protein, C(2)M is expressed in female meiosis and associates with SMC3 (Heidmann et al., 2004). However, transgenic C(2)M lacking its consensus Sse cleavage sites does not appear to prevent meiosis from completing, arguing that C(2)M is not the cleavable component of meiotic cohesin complexes in *Drosophila* (Heidmann et al., 2004). An obvious candidate for the role of meiotic α-kleisin in *Drosophila* is the mitotic paralogue Rad21. However, we found that *Rad21* knockdown does not lead to a detectable loss of cohesion or precocious chromosome segregation in female meiosis (Fig. 6). It is not possible to discount a role for Rad21 in meiotic cohesion based solely on partial knockdown using RNAi. However, we note that with respect to polar body and syncytial mitotic phenotypes, the *Rad21* knockdown appears at least as strong as the *SMC3* knockdown (Fig. 7), yet only SMC3 knockdown affects meiotic cohesion (Fig. 6). Taken together with the complementary findings of Urban et al., 2014, we conclude that Rad21 is not essential for cohesion in *Drosophila* meiosis.

Although we do not know the identity of the α-kleisin component of the *Drosophila* meiotic cohesin complex, there are some candidates: a small number of *Drosophila* genes, *ord*, *solo* and *sunn*, all of which encode non-conserved proteins, display loss-of-function phenotypes indicative of non-disjunction in meiosis I and II, indicating that their protein products are required for meiotic cohesion (Bickel et al., 1997, 2002; Yan et al., 2010; Yan and McKee, 2013; Krishnan et al., 2014). These proteins colocalize and/or physically interact with SMC1 and/or SMC3 in meiosis and, to different degrees, are required for proper loading or maintenance of cohesin components in female meiosis (Khetani and Bickel, 2007; Yan and McKee, 2013; Krishnan et al., 2014). SUNN has some similarity to the stromalin component of cohesin complexes (Krishnan et al., 2014), so by elimination perhaps either Ord or Solo is the Separase-cleavable component of the cohesin complex in *Drosophila* female meiosis.

Sister chromatid cohesion in the polar body

In *Drosophila* female meiosis, the polar body nuclei are not extruded from the egg but instead come together, undergo nuclear envelope breakdown and enter into a mitotic-like arrest with condensed chromosomes arranged on an array of microtubules (Foe et al., 1993). We found that the replicated sister chromatids in the polar body establish cohesion by assembly of cohesin complexes that use SMC3 and Rad21. They gradually lose arm cohesion, in a process that is dependent on Securin destruction and Separase activity, but they maintain centromeric cohesion. This centromeric cohesion might depend on Shugoshin (Mei-S332), which maintains centromeric cohesion prior to anaphase in mitotic cells and until anaphase II in meiotic cells. Shugoshin appears to precisely localize to centromeric regions on polar body chromosomes (Moore et al., 1998), consistent with such a role.

The *Drosophila* egg represents an interesting example of how distinct cell cycle events can occur within a common cytoplasm. As we have shown, cohesion differs temporally – between meiosis and polar body formation (only the latter requiring Rad21), and spatially – between zygote and polar body (only the latter maintaining centromeric cohesion over time) within the same egg. Although there might be little biological importance to the polar body, it might turn out to be a useful model for studying the regulation of cohesion in space and time.

MATERIALS AND METHODS

Drosophila stocks

The following fly stocks were used: *nanos-GAL4 (BDSC#4937)*, *mat-GAL4*, $Rad21^{RNAiGL522}$ and $SMC3^{RNAiGL518}$ (Bloomington *Drosophila* Stock Center), $UASt\text{-}pim^{dba}\text{-}myc$, *UASt-pim-myc* (Leismann and Lehner, 2003). *yw* was used as a wild-type control. Site-directed mutagenesis was performed to generate D-box and KEN-box mutations in *pim*, based on previously generated transgenes (Leismann et al., 2000; Leismann and Lehner, 2003).

Wild-type and altered *pim* sequences were cloned into *pTIGER* (Ferguson et al., 2012) with N-terminal EGFP. Constructs were integrated at attP2 sites (Genetic Services). $Pim^{5'RNAi}$ (5′-CAGCTCACTGCTAGAATTCAA-3′), Sse^{147} (5′-CCCCGAGGCGAAGGAATATAA-3′) and Sse^{213} (5′-CTCAA-TTTACTACCAGGTTAA-3′) were created using the *pVALIUM22* vector using protocols found on the Harvard TRiP website (www.flyrnai.org/TRiP-ACC.html).

Immunostaining and FISH

Fixation and immunostainings were performed using standard methods. *In vitro* activation was performed as in Horner and Wolfner, 2008. FISH was performed as described previously (Dernburg, 2000). The X-cent probe was generated against the 359-bp centromeric repeat on the X-chromosome. The X-arm probe was generated by DOP-PCR amplification of four BACs derived from the distal end of the X-chromosome (clones RP30-G24, RP98-29P19, RP98-805 and RP98-19 from BAC PAC Resources). Probes were end-labelled using Cy3–dUTP (Amersham) or Alexa-Fluor-488–dUTP (Invitrogen). The antibody used was rat anti-Tubulin YL1/2 (Millipore) at 1:500. Secondary antibodies conjugated to Alexa Fluor 488, 568 and 643 were obtained from Invitrogen and used at 1:2000. Oligreen (Invitrogen) was used to stain DNA. Images were acquired as *z*-stacks using an Olympus FV1000 confocal microscope and adjusted only for contrast and brightness in Photoshop.

qRT-PCR, western blotting, immunoprecipitations

Late-stage-enriched oocytes were used for quantitative real-time PCR (qRT-PCR) and Rad21 western blots. Ovaries were dissected in isolation buffer (a hypotonic buffer that does not stimulate egg activation) (Horner and Wolfner, 2008) in the presence of collagenase. Eggs were allowed to settle briefly and smaller, slower-settling egg chambers were removed by aspiration. Settling and aspiration was repeated, resulting in enrichment for late-stage oocytes. For qRT-PCR, mRNA was prepared using RNeasy (Qiagen), first-strand synthesis with revertAID and reactions with SYBR-Green (Life Technologies). *Rp49* was used as a control RNA. Reactions were set up in triplicate and each experiment was performed in triplicate (except for *pim*, which was performed twice). Western blotting for Rad21 was performed on late-stage-enriched oocytes, using rabbit anti-Rad21 antibody (at 1:500 dilution) (Warren et al., 2000) provided by Margarete Heck (University of Edinburgh, Edinburgh, UK). Immunoprecipitation of GFP–Pim was performed using anti-GFP beads (Santa Cruz Biotechnology). Western blots on immunoprecipitates were probed with rabbit anti-Separase (at 1:500 dilution) (Jager et al., 2001) and anti-Pim (at 1:500 dilution) antisera (Stratmann and Lehner, 1996) provided by Christian Lehner (University of Zurich, Zurich, Switzerland).

Acknowledgements

We thank Christian Lehner and Margarete Heck for fly stocks and antisera and Scott Ferguson for the pTIGER plasmid. We thank the Bloomington *Drosophila* Stock Center for fly stocks, TRiP at Harvard Medical School (supported by grant NIH/NIGMS R01-GM084947) for RNAi fly stocks and for the *pValium22* plasmid. We thank Sharon Yong for fly food and members of the Swan lab for helpful discussions.

Competing interests

The authors declare no competing or financial interests.

Author contributions

Experiments were designed by Z.G., O.B. and A.S. Z.G. and O.B. carried out all experiments with help from M.B. and E.F. The paper was written by A.S. with help from Z.G. and O.B.

Funding

This research was supported by a Natural Sciences and Engineering Research Council of Canada (NSERC) discovery grant [grant number 136977 to A.S.].

Supplementary information

Supplementary information available online at
http://jcs.biologists.org/lookup/suppl/doi:10.1242/jcs.179358/-/DC1

References

Bickel, S. E., Wyman, D. W. and OrrWeaver, T. L. (1997). Mutational analysis of the Drosophila sister-chromatid cohesion protein ORD and its role in the maintenance of centromeric cohesion. *Genetics* **146**, 1319-1331.

Bickel, S. E., Orr-Weaver, T. L. and Balicky, E. M. (2002). The sister-chromatid cohesion protein ORD is required for chiasma maintenance in Drosophila oocytes. *Curr. Biol.* **12**, 925-929.

Dernburg, A. (2000). In situ hybridization to somatic chromosomes. In *Drosophila Protocols* (ed. W. Sullivan, M. Ashburner and R. S. Hawley), pp. 25-55. Cold Spring Harbour: Cold Spring Harbour Laboratory Press.

Dernburg, A. F., Sedat, J. W. and Hawley, R. S. (1996). Direct evidence of a role for heterochromatin in meiotic chromosome segregation. *Cell* **86**, 135-146.

Endow, S. A. and Komma, D. J. (1997). Spindle dynamics during meiosis in Drosophila oocytes. *J. Cell Biol.* **137**, 1321-1336.

Ferguson, S. B., Blundon, M. A., Klovstad, M. S. and Schupbach, T. (2012). Modulation of gurken translation by insulin and TOR signaling in Drosophila. *J. Cell Sci.* **125**, 1407-1419.

Foe, V. E. and Alberts, B. M. (1983). Studies of nuclear and cytoplasmic behaviour during the five mitotic cycles that precede gastrulation in Drosophila embryogenesis. *J. Cell Sci.* **61**, 31-70.

Foe, V. E., Odell, G. M. and Edgar, B. A. (1993). Mitosis and morphogenesis in the Drosophila embryo. In *The development of Drosophila melanogaster* (ed. M. Bate and A. Martinez-Arias), pp. 149-300. Cold Spring harbor: Cold Spring Harbor laboratory Press.

Gorr, I. H., Reis, A., Boos, D., Wuhr, M., Madgwick, S., Jones, K. T. and Stemmann, O. (2006). Essential CDK1-inhibitory role for separase during meiosis I in vertebrate oocytes. *Nat. Cell Biol.* **8**, 1035-1037.

Heidmann, D., Horn, S., Heidmann, S., Schleiffer, A., Nasmyth, K. and Lehner, C. F. (2004). The Drosophila meiotic kleisin C(2)M functions before the meiotic divisions. *Chromosoma* **113**, 177-187.

Herbert, M., Levasseur, M., Homer, H., Yallop, K., Murdoch, A. and McDougall, A. (2003). Homologue disjunction in mouse oocytes requires proteolysis of securin and cyclin B1. *Nat. Cell Biol.* **5**, 1023-1025.

Horner, V. L. and Wolfner, M. F. (2008). Mechanical stimulation by osmotic and hydrostatic pressure activates Drosophila oocytes in vitro in a calcium-dependent manner. *Dev. Biol.* **316**, 100-109.

Hughes, S. E. and Hawley, R. S. (2014). Topoisomerase II is required for the proper separation of heterochromatic regions during Drosophila melanogaster female meiosis. *PLoS Genet.* **10**, e1004650.

Jager, H., Herzig, A., Lehner, C. F. and Heidmann, S. (2001). Drosophila separase is required for sister chromatid separation and binds to PIM and THR. *Genes Dev.* **15**, 2572-2584.

Khetani, R. S. and Bickel, S. E. (2007). Regulation of meiotic cohesion and chromosome core morphogenesis during pachytene in Drosophila oocytes. *J. Cell Sci.* **120**, 3123-3137.

Krishnan, B., Thomas, S. E., Yan, R., Yamada, H., Zhulin, I. B. and McKee, B. D. (2014). Sisters unbound is required for meiotic centromeric cohesion in Drosophila melanogaster. *Genetics* **198**, 947-965.

Leismann, O. and Lehner, C. F. (2003). Drosophila securin destruction involves a D-box and a KEN-box and promotes anaphase in parallel with Cyclin A degradation. *J. Cell Sci.* **116**, 2453-2460.

Leismann, O., Herzig, A., Heidmann, S. and Lehner, C. F. (2000). Degradation of Drosophila PIM regulates sister chromatid separation during mitosis. *Genes Dev.* **14**, 2192-2205.

Madgwick, S., Nixon, V. L., Chang, H.-Y., Herbert, M., Levasseur, M. and Jones, K. T. (2004). Maintenance of sister chromatid attachment in mouse eggs through maturation-promoting factor activity. *Dev. Biol.* **275**, 68-81.

Manheim, E. A. and McKim, K. S. (2003). The Synaptonemal complex component C(2)M regulates meiotic crossing over in Drosophila. *Curr. Biol.* **13**, 276-285.

Moore, D. P., Page, A. W., Tang, T. T., Kerrebrock, A. W. and Orr-Weaver, T. L. (1998). The cohesion protein MEI-S332 localizes to condensed meiotic and mitotic centromeres until sister chromatids separate. *J. Cell Biol.* **140**, 1003-1012.

Nasmyth, K. (2002). Segregating sister genomes: the molecular biology of chromosome separation. *Science* **297**, 559-565.

Ni, J.-Q., Zhou, R., Czech, B., Liu, L.-P., Holderbaum, L., Yang-Zhou, D., Shim, H.-S., Tao, R., Handler, D., Karpowicz, P. et al. (2011). A genome-scale shRNA resource for transgenic RNAi in Drosophila. *Nat. Methods* **8**, 405-407.

Page, A. W. and Orr-Weaver, T. L. (1997). Activation of the meiotic divisions in Drosophila oocytes. *Dev. Biol.* **183**, 195-207.

Peters, J.-M. and Nishiyama, T. (2012). Sister chromatid cohesion. *Cold Spring Harb. Perspect. Biol.* **4**, a011130.

Revenkova, E. and Jessberger, R. (2005). Keeping sister chromatids together: cohesins in meiosis. *Reproduction* **130**, 783-790.

Riparbelli, M. G. and Callaini, G. (1996). Meiotic spindle organization in fertilized Drosophila oocyte: presence of centrosomal components in the meiotic apparatus. *J. Cell Sci.* **109**, 911-918.

Staller, M. V., Yan, D., Randklev, S., Bragdon, M. D., Wunderlich, Z. B., Tao, R., Perkins, L. A., DePace, A. H. and Perrimon, N. (2013). Depleting gene activities in early Drosophila embryos with the "maternal-Gal4-shRNA" system. *Genetics* **193**, 51-61.

Stratmann, R. and Lehner, C. F. (1996). Separation of sister chromatids in mitosis requires the Drosophila pimples product, a protein degraded after the metaphase/anaphase transition. *Cell* **84**, 25-35.
Sugimura, I. and Lilly, M. A. (2006). Bruno inhibits the expression of mitotic cyclins during the prophase I meiotic arrest of Drosophila oocytes. *Dev. Cell* **10**, 127-135.
Swan, A. and Schupbach, T. (2007). The Cdc20 (Fzy)/Cdh1-related protein, Cort, cooperates with Fzy in cyclin destruction and anaphase progression in meiosis I and II in Drosophila. *Development* **134**, 891-899.
Tanneti, N. S., Landy, K., Joyce, E. F. and McKim, K. S. (2011). A pathway for synapsis initiation during zygotene in Drosophila oocytes. *Curr. Biol.* **21**, 1852-1857.
Urban, E., Nagarkar-Jaiswal, S., Lehner, C. F. and Heidmann, S. K. (2014). The Cohesin subunit Rad21 is required for synaptonemal complex maintenance, but not sister chromatid cohesion, during Drosophila female meiosis. *PLoS Genet.* **10**, e1004540.
Warren, W. D., Steffensen, S., Lin, E., Coelho, P., Loupart, M.-L., Cobbe, N., Lee, J. Y., McKay, M. J., Orr-Weaver, T., Heck, M. M. S. et al. (2000). The Drosophila RAD21 cohesin persists at the centromere region in mitosis. *Curr. Biol.* **10**, 1463-1466.
Watanabe, Y. (2005). Sister chromatid cohesion along arms and at centromeres. *Trends Genet.* **21**, 405-412.
Weng, K. A., Jeffreys, C. A. and Bickel, S. E. (2014). Rejuvenation of meiotic cohesion in oocytes during prophase I is required for chiasma maintenance and accurate chromosome segregation. *PLoS Genet.* **10**, e1004607.
Yan, R. and McKee, B. D. (2013). The cohesion protein SOLO associates with SMC1 and is required for synapsis, recombination, homolog bias and cohesion and pairing of centromeres in Drosophila Meiosis. *PLoS Genet.* **9**, e1003637.
Yan, R. H., Thomas, S. E., Tsai, J.-H., Yamada, Y. and McKee, B. D. (2010). SOLO: a meiotic protein required for centromere cohesion, coorientation, and SMC1 localization in Drosophila melanogaster. *J. Cell Biol.* **188**, 335-349.